




## Overconsolidated flysch-type clays. Engineering considerations for the Strait of Gibraltar tunnel project

Francisco Javier Manzano<sup>1#</sup> , Francisco Lamas<sup>2</sup> , José Miguel Azañón<sup>3</sup> 

Article

### Keywords

Flysch clay  
Gibraltar Strait tunnel  
Cam clay model  
Triaxial testing  
Hardening Soil model  
Soil modelling

### Abstract

The stress-strain behaviour of 85 overconsolidated clay samples from Campo de Gibraltar Flysch Through Domain (Algeciras Unit, South Spain) is presented and discussed. The samples were identified and classified following ASTM standards while their chemical and mineralogical composition were determined by chemical and X-ray techniques. Several samples were tested under triaxial as well as oedometric conditions. Given the results, a detailed comparison was made between different theoretical constitutive models and real testing data, using the finite-elements method. The comparison indicated a good fit between experimental data and those found with finite-elements modelling when the Hardening Soil constitutive model was used. This model showed a better fit than did the Modified Cam-Clay model (historically used for modelling clayey soils), although the latter fit proved better for lower strain values (<5%) than higher ones. These results clarify this intermediate material (hard soils – weak rocks) behaviour and will help in Strait of Gibraltar tunnel project design, as these materials are widely involved in this tunnel design.

## 1. Introduction

Joining Africa and Europe by a tunnel under the Strait of Gibraltar is a longstanding idea from the 19th century, first appearing as a project in documents related to Charles Villedieu in 1869 (Velasco, 2016). Since then, various plans had been proposed until 1995, when the latest proposal was finally submitted. This project consists of a single railway tunnel running from Punta Paloma (Spain) to Punta Malabata (Morocco), which would be completed by a second tunnel in a subsequent stage (Figure 1).

This huge engineering project would involve a complex geological scheme associated with flysch-type deposits (Manzano et al., 2020).

The Campo de Gibraltar Flysch Trough Domain represents part of the Gibraltar Arc System, which is in turn formed by Betic System, the Rift, and the Alboran Basin. Formed during Alpine orogenesis in the Betic Cordillera, it is widely represented in southern Spain and northern Morocco. Lithologically, it has mainly deep marine facies with multicoloured clays (often marls) and carbonatic siliciclastic sandstones, typical of flysch-type deposits (Balanyá et al., 2004).

The term “flysch”, introduced by Studer (1827), has historically been used by Alpine geologists to define “sedimentary deposits consisting in varying alternation

of clastic sediments associated with orogenesis” (Marinos & Hoek, 2001). These deposits are formed by a rhythmic alternation of fine-grained materials and sandstone layers. Geotechnically, these formations are characterised by their diversity, clay-mineral content, and several sheared discontinuities.

Despite the existence of wide outcrops of flysch worldwide and the complexity of studying their behaviour, relatively little research has been conducted in this field, despite the fact that these formations pose several critical engineering problems for public works (Palomba et al., 2013; Dounias et al., 1996). Over-consolidated clays related to flysch deposits are widely recognized to be involved in several engineering problems. Slope instabilities associated with such deposits are well known throughout the world (Mikoš et al., 2009; Arbanas et al., 2008; Azañón et al., 2010; Pánek et al., 2009, etc). Landslides constitute the main hazard related to flysch deposits though not the only one. Coastal cliff retreats (Moon & Healy, 1994), or the complexities of tunnel support (Jovičić et al, 2009; Aydin et al., 2004) are some of the problems caused by these deposits. All of these hazards together require fuller knowledge of this special soft rock- hard soil deposits.

In particular, the study of the behaviour of Campo de Gibraltar Flysch clays (Betic Cordillera, southern Spain) has led engineering geologists to propose an approach for

#Corresponding author. E-mail address: franciscojavier.manzano@uca.es

<sup>1</sup>Universidad de Cádiz, Escuela Politécnica Superior, Departamento de Ingeniería Civil e Industrial, Algeciras, Cádiz, España.

<sup>2</sup>Universidad de Granada, Escuela Técnica Superior de Ingeniería de Caminos Canales y Puertos, Departamento de Ingeniería Civil, Granada, España.

<sup>3</sup>Universidad de Granada, Facultad de Ciencias, Departamento de Geodinámica, Granada, España.

Submitted on February 20, 2022; Final Acceptance on November 21, 2022; Discussion open until May 31, 2023.

<https://doi.org/10.28927/SR.2023.002222>



This is an Open Access article distributed under the terms of the Creative Commons Attribution License, which permits unrestricted use, distribution, and reproduction in any medium, provided the original work is properly cited.

analysing such complex soils, which show intermediate behaviour between hard soils and soft rocks. This soil presents serious difficulties for taking good-quality samples (Arbanas et al., 2008). For example, soil samples often become disturbed and must be tested in a short period of time (Roje-Bonacci, 1998).

The present paper highlights a case study in southern Spain with the aim of improving knowledge of Flysch soil characteristics by presenting the results of several intensive soil investigations in different locations within Campo de Gibraltar Trough Domain. A full set of mechanical and chemical testing is presented and discussed. These tests allowed us to understand this soil behavior and suppose a better knowledge of such complex and uninvestigated soils. This has major implications for future engineering projects,

including tunnel under the Strait of Gibraltar as its design will strongly be affected by geotechnical characteristics of these soils.

## 2. Sampling, laboratory testing methods, and results

### 2.1 Sampling and samples

Map of Figure 2 shows the locations of the samples used in this study. A total of 85 samples were tested, all taken as undisturbed as possible according to ASTM D1587 (ASTM, 2000). When undisturbed sampling was not feasible or samples



Figure 1. Tunnel layout proposal. Red line shows new proposal whereas blue one shows previous one.

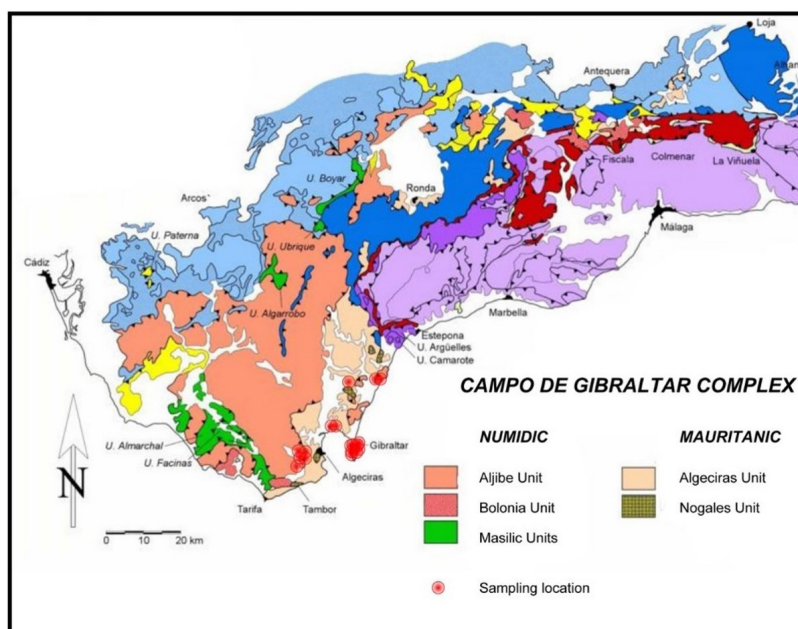


Figure 2. Geological plan of the study area showing sampling locations.

**Table 1.** Samples depth.

Sample	Depth	Sample	Depth	Sample	Depth
TES-01-12	4.60 - 5.00	TES 34-12	8.60 - 9.00	TES 26-13	19.00-19.60
TES-02-12	10.30 - 10.60	TES 35-12	7.15 - 7.96	TES 27-13	16.00-17.00
TES-03-12	11.60 - 12.00	TES 36-12	5.60 - 5.90	TES 28-13	4.80 - 5.20
TES-04-12	14.25 - 14.65	TES 01-13	12.20 - 12.45	TES 29-13	8.80 - 9.20
TES-08-12	10.60 - 11.00	TES 02-13	3.00 - 3.60	TES 30-13	12.20 - 12.50
TES-10-12	8.40 - 8.65	TES 03-13 (SR)	6.10 - 6.70	TES 31-13	7.00 - 7.33
TES-11-12	12.60 - 12.85	TES 03-13 (M)	6.70 - 7.30	TES 32-13	5.30 - 5.90
TES-12-12	16.10 - 16.30	TES 04-13	8.90 - 9.30	TES 33-13	19.00 - 19.40
TES 13-12	5.10 - 5.40	TES 05-13	14.20 - 14.5	TES 34-13	7.80 - 8.15
TES 14-12	3.60 - 3.90	TES 06-13	15.35 - 15.70	TES 37-13	10.00 - 10.30
TES 15-12	9.85 - 10.10	TES 07-13	8.70 - 9.00	TES 35-13	10.50 - 11.00
TES 16-12	8.50 - 8.80	TES 08-13	10.10 - 10.60	TES 36-13	11.25 - 11.80
TES 17-12	7.30 - 7.70	TES 09-13	14.25 - 14.55	TES 01-14	7.35 - 7.8
TES 18-12	13.75 - 14.00	TES 11-13	1.20 - 1.80	TES 02-14	10.8 - 11.23
TES 19-12	7.70 - 8.30	TES 12-13	5.0 - 5.6	TES 03-14	6.1 - 6.5
TES 20-12	14.10 - 14-35	TES 13-13	7.5 - 8.1	TES 04-14	8.10 - 8.70
TES 21-12	14.10 - 14-35	TES 14-13	10.80 - 11.12	TES 05-14	16.75 - 17.10
TES 22-12	15.00 - 15.40	TES 15-13	3.0 - 3.3	TES 06-14	10.95 - 11.90
TES 23-12	4.75 - 5.00	TES 16-13	8.3 - 8.6	TES 07-14	18.20 - 18.57
TES 24-12	6.55-6.75	TES 17-13	3.35 - 3.9	TES 08-14	22.90 - 23.27
TES 25-12	19.6 - 20.00	TES 18-13	4.1 - 4.4	TES 09-14	4.00 - 4.45
TES 26-12	14.7 - 15.10	TES 19-13	16.9 - 17.5	TES 10-14	6.20 - 6.60
TES 27-12	28.00 - 28.40	TES 20-13	16.13 - 16.60	TES 11-14	1.98 - 2.50
TES 28-12	16.10-16.35	TES 21-13	18.90 - 19.34	TES 12-14	9.20 - 9.50
TES 29-12	9.00 - 10.00	TES 22-13	18.40-18.84	TES 13-14	4.60 - 5.00
TES 30-12	10.00 - 11-00	TES 23-13	15.20-15.60	TES 15-14	2.85 - 3.60
TES 31-12	6.50-7.50	TES 24-13	17.00-17.60	TES 18-14	7.00 - 7.37
TES 32-12	4.50 - 5.50	TES 25-13	17.48-17.80	TES 19-14	9.20 - 9.60
TES 33-12	9.00 - 10.00				

were of poor quality, a triple barrel was used to obtain good quality cores that could be tested in the laboratory. Samples were obtained at different depths in each location (Table 1)

All samples were taken in soils belonging to Algeciras Unit which is the upper unit within Mauritanian facies of Campo de Gibraltar flysh domain. This unit is aged from upper cretacic to Neogene and it is characterized by a rhythmic alternance of sandstones and overconsolidated hard clays. These clayey levels were sampled for further laboratory testing.

## 2.2 Sample description: phase relationships, particle size, and composition

All the samples were taken for laboratory testing. Geotechnical characterization followed ASTM standards (Table 2) for different parameters and variables.

Table 3 presents data concerning the natural moisture, percentage of particle sizes below 0.08 mm, and Atterberg consistency parameters: liquid limit (LL), plastic limit (PL), and plasticity index (PI).

**Table 2.** Standards used for soil testing.

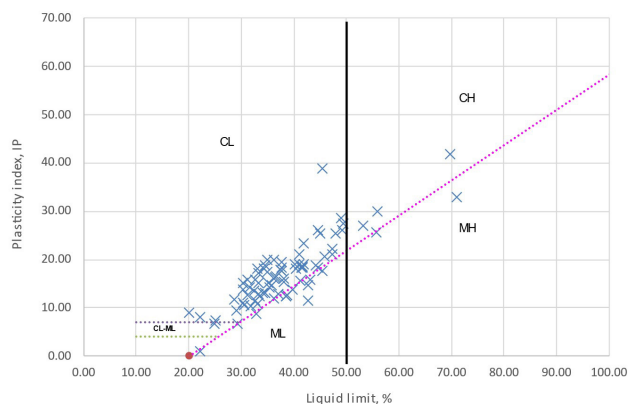
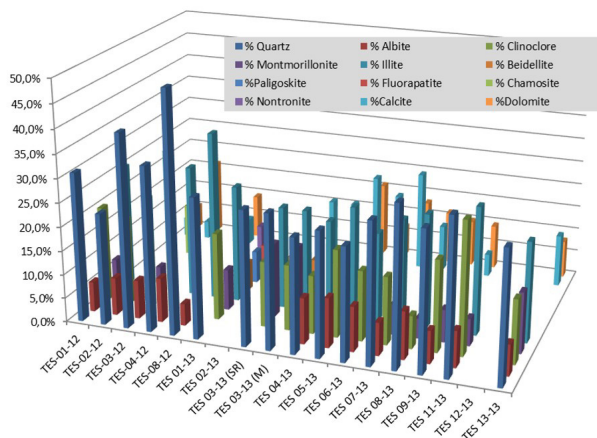
Test	ASTM Standard
Sieving Analysis	D 6913
Atterberg Limits	D 4318
Moisture	D 4959
Density	D 7263
Soil classification	D 2487
Triaxial tests	D 4767, D 7181, D2850
Oedometric test	D 2435
Organic matter content	D 2974
SO4 content	C 1580
CO3 content	D 4373
Soluble salts content	D 4542

Most of the samples could be classified as inorganic low-plasticity clays of the CL type, in accordance with the Unified Soil-Classification System (Figure 3). Only three samples were classified as high-plasticity clays (CH), three as CL-ML soils, and five as a low-plasticity mud (ML).

**Table 3.** Classification tests results.

	$w$	$F_c$	$LL$	$PL$	$PI$	$\gamma'$	$\gamma_d$
Maximum	34.00	100.00	70.80	37.90	41.80	2.34	2.10
Mean	15.73	69.92	38.19	21.13	17.54	2.05	1.78
Minimum	5.50	28.30	20.00	6.70	6.60	1.74	1.45
Standard Dev.	5.34	19.39	8.83	4.63	7.07	0.14	0.16

$w$  = Moisture Content, %;  $FC$  = %<0,08;  $LL$  = Liquid Limit;  $PL$  = Plastic Limit;  $PI$  = Plasticity Index;  $\gamma'$  = Apparent Density;  $\gamma_d$  = Dry Density.

**Figure 3.** Plasticity chart showing test results.**Figure 4.** Mineralogical composition of the samples analysed.

For a mineralogical characterization of the clay samples, X-ray diffraction analyses were made on 16 samples. A powder aggregate prepared by milling was placed in the XR equipment, using a test with a speed of 2°/min and a wavelength of 1.5405 nanometres. The results were interpreted using X Powder software (Martín-Ramos, 2004). Figure 4 shows the mineralogical distribution of samples analysed, indicating that the main component was invariably quartz, with a high percentage of illite. Calcite and dolomite were also major constituents while albite, montmorillonite, and clinoclore also

registered significant percentages. The minor constituents of these clays were beidellite, paligorskite, fluorapatite, chamosite, and nontronite.

The chemical composition was established both by analytical methods following the usual standards (Table 2) and by X-ray fluorescence. The latter is also an analytical technique based on measuring intensities that can later be translated into component concentrations. In this method, a continuous spectrum of characteristic radiation is sent from the equipment to the sample, producing primary fluorescent radiation which produces an X-ray emission that can be analysed. A Brunker spectrometer (model S4 Pioneer) was used, equipped with a Rh tube (60 kV; 150 mA) having a detection limit from 0.1 to 10 ppm.

With the analytical methods applied, the percentages of sulphates, total carbonates, soluble salts and organic matter were calculated whereas X-ray fluorescence showed a screening of chemical elements (expressed as oxide percentages) in the samples. Table 4 presents the results of both analyses. These results are consistent with the mineralogy of the samples where quartz was the main mineral phase.

As a complement to the chemical and mineralogical tests, five undisturbed samples were analyzed using SEM (Carl Zeiss Scanning Electron Microscope, model ULTRA 55). Those samples were dried at 50°C to avoid losing the inner water content. Then, samples were prepared using gold powder to improve their electrical conductivity to ensure the clearest possible images. Due to the low electrical conductivity of the samples, 2 keV of acceleration potential of the electron beam was used with a working distance of 2-4 mm. A secondary electron detector was used to determine the crystalline structure of minerals and their texture.

Figure 5 (a, b, c, d and e) indicate images showing the soil texture and the mineralogical assemblages of those undisturbed samples. As reflected in the figure, almost no organic clastic pieces can be found (only three microfossils were found in all the images), compatible with low to medium carbonate content in these samples. The phyllosilicates showed a medium to open texture, which could explain the medium to high swelling behaviour found in these samples. Also, in Figure 5c and 5d, the grains have a laminar, non-rounded shape for phyllosilicates and a rounded shape for quartz grains. No marked differences were detected between the samples analyzed.



## 2.3 Oedometric and triaxial tests

52 Oedometer tests were performed to establish consolidation coefficients. These results (Table 5) are reported in terms of lambda ( $\lambda$ ) and kappa ( $\kappa$ ), following methodology described in Cam Clay models methodology (Schofield, 1993).

Given the low permeability of the soil samples tested and their behavior as cohesive undrained soils, undrained triaxial CU tests with pore pressure measurement were considered the best approach to the in situ stress-strain behavior. A total of 57 triaxial tests (9 drained and 48 undrained) were conducted on undisturbed samples. All tests (stress controlled) were carried out using usual chamber pressures of 650, 750 and

900 kPa and back pressure of 600 kPa. All samples were fully saturated as a first stage of the testing.

Table 5 lists the values of cohesion and friction angle determined in the triaxial tests (minimum, maximum and mean values).

## 3. Results discussion

### 3.1 Soil nature, phase relationship, particle size and composition.

The samples analysed were mainly low-plasticity clays of the group CL in the Unified Soil Classification System

**Table 4.** Results of the chemical composition analysis.

	X-ray diffraction results										Analytical results			
	SiO <sub>2</sub>	Al <sub>2</sub> O <sub>3</sub>	Fe <sub>2</sub> O <sub>3</sub>	MnO	MgO	CaO	Na <sub>2</sub> O	K <sub>2</sub> O	TiO <sub>2</sub>	P <sub>2</sub> O <sub>5</sub>	Soluble salts	Sulphates	Organic Matter	Carbonates
TES-01-12	51.67	21.61	6.37	0.03	2.37	1.50	0.26	3.17	0.96	0.10	0.00	0.00	1.11	4.47
TES-02-12	50.39	20.21	6.80	0.37	3.26	2.84	0.66	3.46	0.82	0.16	0.00	0.00	0.80	8.06
TES-03-12	46.68	17.52	6.82	0.15	3.74	8.95	0.84	3.30	0.77	0.28	0.00	0.00	0.66	2.10
TES-04-12	51.06	19.51	8.05	0.25	3.11	2.36	0.71	3.65	0.83	0.17	0.00	0.01	0.37	3.89
TES-08-12	56.38	19.08	7.46	0.11	2.41	1.61	0.93	3.39	0.84	0.82	0.00	0.00	0.21	1.52
TES 01-13	50.97	20.18	7.09	0.04	1.74	1.94	0.45	2.30	0.94	0.18	0.00	0.00	0.00	5.99
TES 02-13	51.87	20.51	7.40	0.03	1.69	1.44	0.50	2.27	0.97	0.19	0.00	0.32	0.33	2.20
TES 03-13 (SR)	0.48	16.40	7.14	0.07	2.06	6.74	0.47	1.91	0.92	0.39				
TES 04-13	45.43	16.93	6.40	0.08	3.71	9.17	0.91	3.18	0.76	0.12	0.00	0.00	0.45	16.44
TES 05-13	0.44	15.56	7.28	0.12	3.46	10.73	0.78	3.09	0.75	0.12				
TES 06-13	0.42	15.73	6.76	0.10	3.20	11.26	0.64	3.16	0.78	0.12	0.00	0.00	0.00	7.81
TES 07-13	44.33	18.51	6.62	0.06	3.00	7.99	0.47	2.86	0.97	0.10	0.00	0.00	0.21	7.82
TES 08-13	42.00	15.65	6.13	0.12	3.62	12.79	0.80	2.95	0.73	0.11	0.00	0.00	0.00	1.52
TES 09-13	49.90	18.89	8.60	0.30	3.01	2.53	0.66	3.86	0.89	0.16				
TES 11-13	50.86	21.52	8.71	0.03	1.81	0.83	0.58	2.45	1.19	0.18	0.00	0.00	0.66	9.30
TES 13-13	44.00	19.12	6.04	0.05	2.52	8.74	0.54	2.33	0.94	0.11	0.00	0.00	0.70	15.81
TES 20-13											0.32	0.00	0.25	0.16
TES 21-13											0.20	0.00	0.28	0.16
TES 22-13											0.32	0.00	0.29	0.24
TES 23-13											0.23	0.00	0.23	0.23
TES 24-13											0.54	0.00	0.41	4.30
TES 25-13											0.04	0.00	0.32	3.00
TES 26-13											0.46	0.00	0.61	9.80
TES 27-13											0.44	0.00	0.32	1.80
Minimum	0.42	15.56	6.04	0.03	1.69	0.83	0.26	1.91	0.73	0.10	0.00	0.00	0.00	0.16
Mean	39.80	18.56	7.10	0.12	2.79	5.71	0.64	2.96	0.88	0.21	0.12	0.02	0.39	5.08
Maximum	56.38	21.61	8.71	0.37	3.74	12.79	0.93	3.86	1.19	0.82	0.54	0.32	1.11	16.44
Standard Dev.	19.86	2.04	0.80	0.10	0.71	4.20	0.19	0.56	0.12	0.18	0.19	0.07	0.28	4.82

**Table 5.** Oedometric and Triaxial test results. Note minimum value of friction angle was obtained in a anomalous testing result (TES-23-12).

	$c'$ (kPa)	$\phi'$ (°)	$\lambda$	$\kappa$	$e_i$
Maximum	150.00	49.60	0.130	0.041	0.760
Mean	36.24	26.75	0.050	0.013	0.492
Minimum	0.00	6.84	0.007	0.000	0.107
Standard Dev.	35.03	8.30	0.023	0.009	0.156

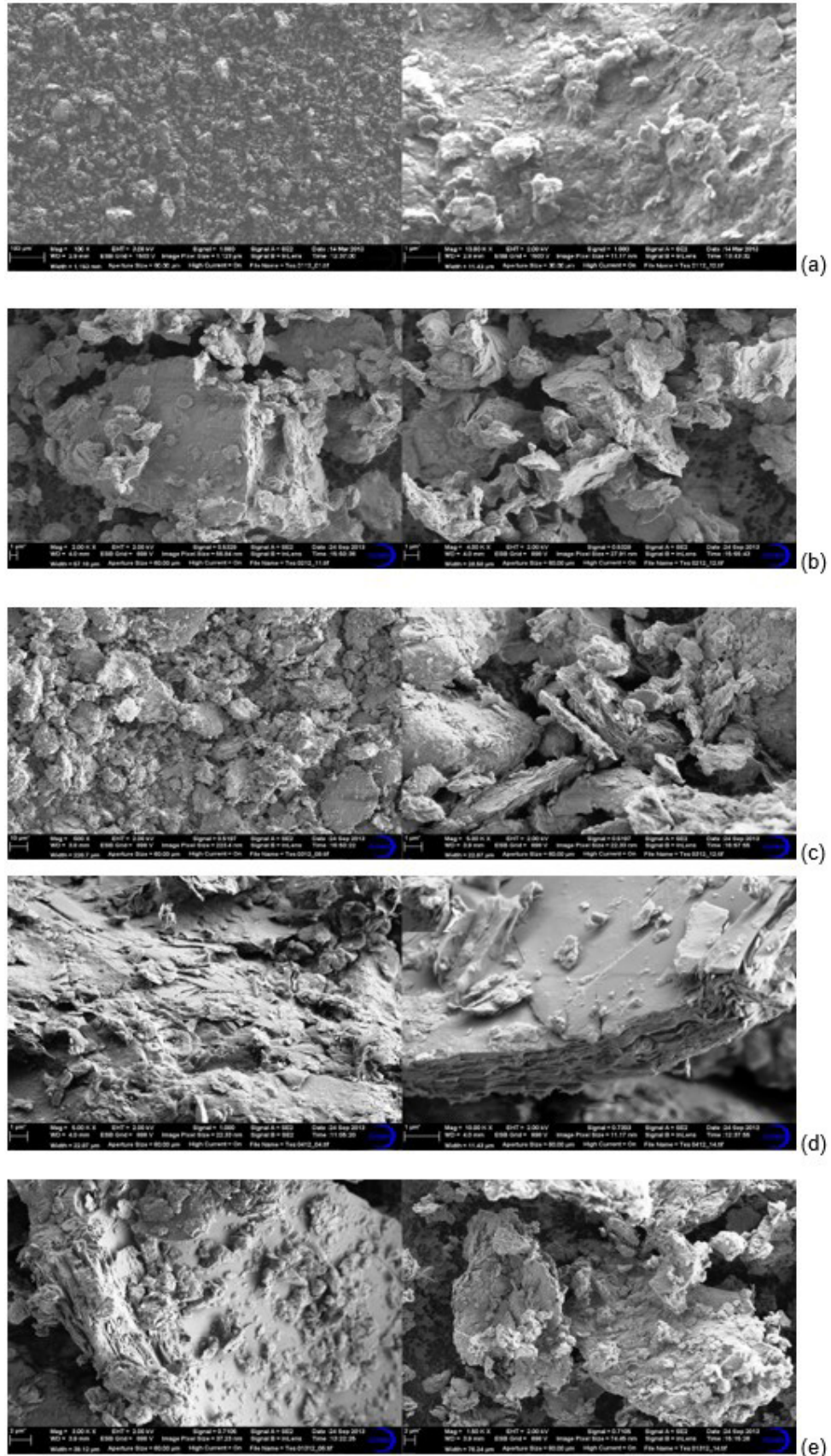


Figure 5. SEM image of samples: (a) TES 001/12; (b) TES 002/12; (c) TES 003/12; (d) TES 004/12; (e) TES 005/12.

for Engineering Purposes (ASTM, 2011). Only 11 samples were not classified as CL (3 samples classified as CH, 3 as CL-ML, and 5 as ML).

The samples proved highly homogeneous in terms of particle-size distribution and had no significant gravel content but a high content in particles smaller than 0.08 mm (mean value = 69.92%; standard deviation = 19.39). Regarding the clay-silt differentiation, the 23 sedimentation-analysis tests undertaken indicated a substantial percentage of silt in the fraction smaller than 0.08 mm (in some cases even higher than the clay percentage), indicating low activity in those samples (Figure 6) according to the Skempton activity criteria (Skempton, 1953).

Table 4 shows the chemical composition established by X-ray diffraction and analytical methods. The carbonate content (which could influence the geotechnical behavior of these soils), was found to range from 0.16 to 34.72 with a mean value of 10.29 (standard deviation = 9.87). The highest percentages corresponded to aluminum and silica (the majority component being quartz).

Regarding the mineralogical composition, as expected, clay minerals were not main component. In all cases the main component was quartz, followed by a substantial percentage of illite. Calcite and dolomite were also major constituents, with albite, montmorillonite, and clinoclore in significant percentages. This mineralogical composition, with almost no skeletal grains in its composition, accounts for the medium to low carbonate content (mean value under 15%) even when those soils were formed in an environment where the carbonate content could be expected to be higher. Also, illite and montmorillonite in the samples explain the swelling behaviour, which was medium to high in some of the samples and well known in these soils (Azañón et al., 2010).

### 3.2 Stress-strain relationships

#### 3.2.1 Oedometric and triaxial behaviour

For an understanding and characterisation of soil behaviour under uniaxial oedometric compression, 52 oedometric tests were undertaken. In all cases, the oedometric coefficients were reduced following Critical State methodology (Schofield, 1993) in terms of lambda and kappa. Table 5 shows the results, which establish a low compressibility in noval loading, with a mean lambda value of 0.050 (standard deviation = 0.023). The kappa mean value was 0.013 (standard deviation = 0.009) and the initial void ratio had a mean value of 0.492 with a standard deviation of 0.156.

The results reflected a stiff soil with low compressibility indexes and an initial void ratio notably lower than expected.

Some additional facts should be highlighted regarding behaviour under triaxial compression. All tests showed a homogeneous behaviour under triaxial compression. Firstly, almost all the samples showed a progressive hardening under

strain, this being more notable for higher chamber pressures but also recognizable at low pressures (Figure 7, 8 & 9). Secondly, in relation to the pore pressure, in almost all cases, the pore pressure increased until a peak value was reached in the test, at which point values started to decrease until failure (Figure 10). This demonstrates an important aspect of the behavior of the soil: the pore pressure led to suction in many cases whereas vertical effective pressure continued to augment. Also noticeable is the behavior in a p-q diagram, showing a clear linear trend (Figure 7) with a high  $R^2$  value ( $R^2=0.96$ ).

## 4. Soil modelling

Once all the tests were analyzed and soil parameters estimated, comparisons were made among the experimental

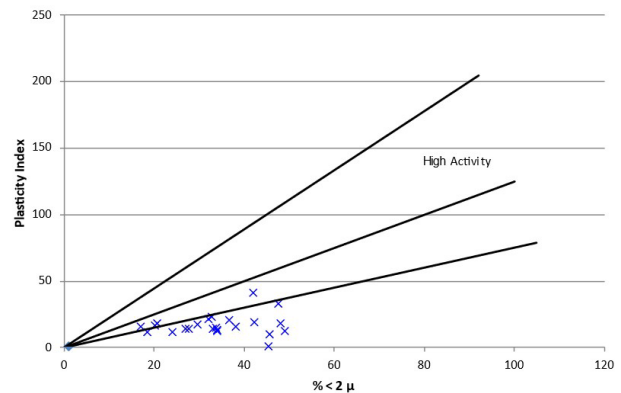


Figure 6. Activity chart.

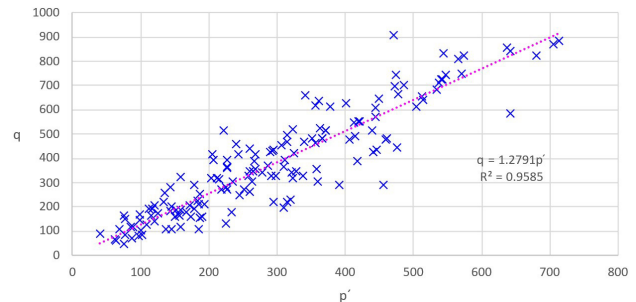


Figure 7. Failure data ( $q/p_e$  vs  $p/p_e$ ).

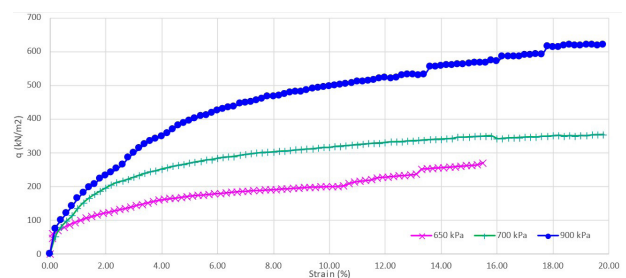


Figure 8.  $q$  vs. strain obtained for different chamber pressures. Graph shows mean value of all tests.



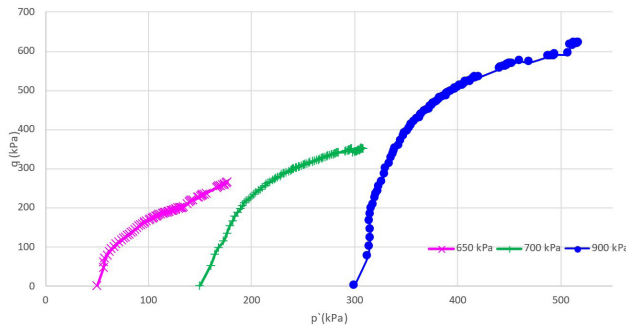


Figure 9.  $p'$ - $q$  diagram (mean values) for different chamber pressures.

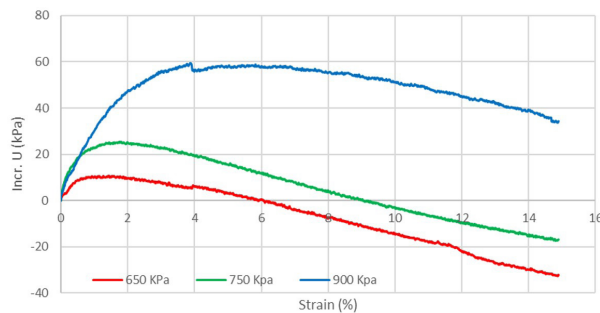


Figure 10. Mean values of pore pressure increments during testing.

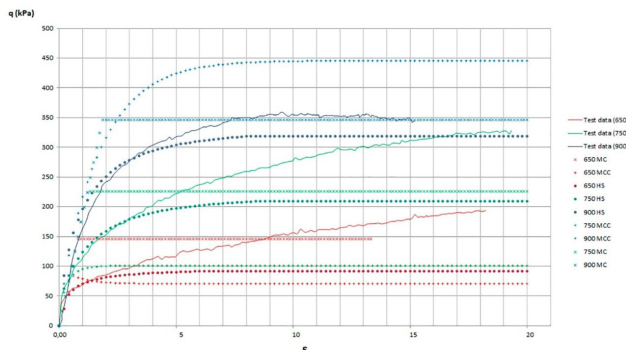


Figure 11. Triaxial testing and finite-elements model comparison.

data and theoretical models. The comparisons were undertaken by modelling the triaxial test using the soil-testing tool of Plaxis 2D software. This tool enables virtual soil modelling under the same conditions used for real laboratory testing and then allows the results to be compared. Each soil test was modelled using Mohr-Coulomb, Modified Cam-Clay, and Hardening Soil models (Plaxis, 2014). Mohr-Coulomb was selected for being the most widely used model in initial approaches to engineering problems whereas Modified Cam-Clay was selected for being broadly applied for clay modelling. On the other hand, the Hardening Soil constitutive model was selected in order to check its feasibility for accurate modelling the behaviour of this soil. Parameters used for soil modelling correspond to mean values shown in Table 5.

The results for each constitutive model vs. real test data were plotted in terms of deviatoric stress and strain, and the findings were analyzed to establish whether these constitutive models were consistent with real soil behavior. The Hardening Soil model best fit real lab testing, with a better fit for chamber pressures of 650 and 750 kPa (Figure 11). In any case, the correlation was good for strain values under 5 in all cases. For strain values from 5% to 15%, the model fit the test results except for chamber pressure equal to 900 kPa.

## 5. Conclusions

A full set of laboratory testing was conducted on 83 clay samples taken in the Campo de Gibraltar Flysch Trough Domain related to the material that will be found during Gibraltar Strait Tunnel. These tests showed these clays to be of low plasticity with quartz consistently as the main component, followed by a high percentage of illite (albite, montmorillonite, and clinoclore also registering notable percentages). Oedometric testing revealed these clays to be a stiff soil with low compressibility indexes and a low initial void ratio (mean  $\lambda$  value of 0.050 with a standard deviation = 0.023; mean  $\kappa$  value = 0.013 with standard deviation of 0.009 and initial mean void ratio of 0.492 with a standard deviation of 0.156). With respect to behavior under triaxial compression tests, the cohesion found indicates high variability between 0 and 150 kPa (mean value = 36.24 kPa; standard deviation = 35.03) whereas the friction angle showed a more homogeneous value (mean value = 26.75°; standard deviation = 6.84). The samples tested showed a progressive hardening with strain and also indicated that the pore pressure led to suction in many cases, whilst vertical effective pressure was still increasing.

A good fit of the laboratory testing results with finite-element modelling when the Hardening Soil constitutive model was used was clearly established. This constitutive model fits real results better than does the Modified Cam-Clay model, although it has been used for typical clays (Roscoe & Burland, 1968; Burland, 1990; Wood, 1990). The Theoretical Hardening soil model fit the laboratory testing values better at low strain values (<5%), this constituting a crucial issue to be taken into account when model data are analyzed in engineering practice.

## Acknowledgements

The authors thank Sergeyco Andalucía S.L. for funding all the tests included in this paper and SECEGSA for allowing access to their entire database. Appreciation also goes to Mr. Juan Almagro and Mr. Andres Núñez (Acerinox Europe) for their aid with Scanning Electronic Microscopy images and Mr. Michael Millgate for reviewing the language of the text.



## Declaration of interest

The authors have no conflicts of interest to declare. All co-authors have observed and affirmed the contents of the paper and there is no financial interest to report.

## Authors' contributions

Francisco Javier Manzano: conceptualization, investigation, software, writing original draft preparation, reviewing and editing. Francisco Lamas: conceptualization, methodology, validation, data curation. José Miguel Azañón: supervision.

## Data availability

The datasets generated analyzed in the course of the current study are available from the 267 corresponding author upon request.

## List of symbols

$c'$	Effective cohesion.
$e_i$	Initial void ratio.
$p'$	Mean effective stress.
$q$	Deviatoric stress.
$q/p_e$	Normalized mean effective stress.
$q/p'_e$	Normalized deviatoric stress.
$w$	Moisture content (%).
$^{\circ}\text{C}$	Degrees centigrade.
$FC$	Fines content (particles lower than 0.08 mm).
$HS$	Hardening Soil constitutive model.
$LL$	Liquid Limit.
$MC$	Mohr Coulomb constitutive model.
$MCC$	Modified Cam Clay constitutive model.
$PL$	Plastic limit.
$PI$	Plasticity index.
$SEM$	Scanning electronic microscope.
$\gamma'$	Apparent Density.
$\gamma_d$	Dry Density.
$\varepsilon$	Strain.
$\kappa$	Kappa parameter (Wood, 1990).
$\lambda$	Lambda parameter (Wood, 1990).
$\phi'$	Effective friction angle.

## References

- Arbanas, Ž., Grošić, M., & Briški, G. (2008). Behaviour of Engineered Slopes in Flysch Rock Mass. In *Proceedings of the 1st Southern Hemisphere International Rock Mechanics Symposium (SHIRMS)* (pp. 403-504). Australia: Australian Centre for Geomechanics. [https://doi.org/10.36487/ACG\\_repo/808\\_07](https://doi.org/10.36487/ACG_repo/808_07)
- ASTM D1587. (2000). *Standard Practice for Thin-Walled Tube Sampling of Soils for Geotechnical Purposes*. ASTM International, West Conshohocken, PA.
- ASTM D2487. (2011). *Standard Practice for Classification of Soils for Engineering Purposes (Unified Soil Classification System)*. ASTM International, West Conshohocken, PA.
- Aydın, A., Ozbek, A., & Cobanoğlu, I. (2004). Tunnelling in difficult ground: a case study from Dranz tunnel, Sinop, Turkey. *Engineering Geology*, 74(3-4), 293-301. <http://dx.doi.org/10.1016/j.enggeo.2004.04.003>.
- Azañón, J.M.A., Antonio, A., Yesares, J., Tsige, M., Mateos, R.M., Nieto, F., Delgado, J., López-Chicano, M., Martín, W., & Rodríguez-Fernández, J. (2010). Regional-scale high-plasticity clay-bearing formation as controlling factor on landslides in Southeast Spain. *Geomorphology*, 120(1-2), 26-37. <http://dx.doi.org/10.1016/j.geomorph.2009.09.012>.
- Balanyá, J.C., Crespo-Blanc, A., Esteras, M., Luján, M., Martín Algarra, A., & Martín-Martín, M. (2004). Complejo del campo de Gibraltar. In J.A. Vera (Ed.), *Geología de España* (pp. 384-395). Instituto Geológico y Minero de España.
- Burland, J.B. (1990). On the compressibility and shear strength of natural clays. *Geotechnique*, 40(3), 329-378. <http://dx.doi.org/10.1680/geot.1990.40.3.329>.
- Dounias, G.P.P., Marinos, P., & Vaughan, P. (1996). Landslide reactivation in flysch colluvial at the Evinos dam site. In *Proceedings of the 7th International Symposium on Landslides* (pp. 201-206). Trondheim: Balkema.
- Jovičić, V., Šušteršič, J., & Vukelić, Ž. (2009). The application of fibre reinforced shotcrete as primary support for a tunnel in flysch. *Tunnelling and Underground Space Technology*, 24(6), 723-730. <http://dx.doi.org/10.1016/j.tust.2009.05.003>.
- Manzano, F.J., Lamas, F., & Azañón, J.M. (2020). Geotechnics as a conditioning factor in large infrastructures. The link Europe–Africa. *Ciudad y Territorio Estudios Territoriales*, 52(206), 739-752. <http://dx.doi.org/10.37230/CyTET.2020.206.02>.
- Marinos, P., & Hoek, E. (2001). Estimating the geotechnical properties of heterogeneous rock masses such as flysch. *Bulletin of Engineering Geology and the Environment*, 60(2), 85-92. <http://dx.doi.org/10.1007/s100640000090>.
- Martín-Ramos, J.D. (2004). *X-Powder, a software package for powder X-ray diffraction analysis*. Retrieved in February 20, 2022, from <http://www.xpowder.com>.
- Mikoš, M., Petkovšek, A., & Majes, B. (2009). Mechanisms of landslides in over-consolidated clays and flysch. *Activity scale and targeted region: national. Landslides*, 6(4), 367-371.
- Moon, V.G., & Healy, T. (1994). Mechanisms of coastal cliff retreat and hazard zone delineation in soft flysch deposits. *Journal of Coastal Research*, 10 (3), 1994, pp 663–680. *International Journal of Rock Mechanics and Mining Sciences & Geomechanics Abstracts*, 31(6), 267-268. [http://dx.doi.org/10.1016/0148-9062\(94\)90051-5](http://dx.doi.org/10.1016/0148-9062(94)90051-5).
- Palomba, M.R.G., Amadini, F., Carrieri, G., & Jain, A.R. (2013). Chenani-Nashri Tunnel, the longest road tunnel in India: a challenging case for design-optimization during construction. In *World Tunnel Congress 2013*.

- Underground - the way to the future!* (pp. 964-971). Geneva: Taylor & Francis Group.
- Pánek, T., Hradecký, J., Minár, J., Hungr, O., & Dušek, R. (2009). Late Holocene catastrophic slope collapse affected by deep-seated gravitational deformation in flysch: ropice Mountain, Czech Republic. *Geomorphology*, 103(3), 414-429. <http://dx.doi.org/10.1016/j.geomorph.2008.07.012>.
- Plaxis. (2014). *Material Models Manual*. Retrieved in February 20, 2022, from [https://communities.bentley.com/cfs-file/\\_key/communityserver-wikis-components-files/00-00-00-05-58/0118.PLAXIS3DCE\\_2D00\\_V20.02\\_2D00\\_3\\_2D00\\_Material\\_2D00\\_Models.pdf](https://communities.bentley.com/cfs-file/_key/communityserver-wikis-components-files/00-00-00-05-58/0118.PLAXIS3DCE_2D00_V20.02_2D00_3_2D00_Material_2D00_Models.pdf).
- Roje-Bonacci, T. (1998). Parameter changes after weathering of soft rock in flysch: the geotechnics of hard soils - soft rocks. In *Proceedings of the second international symposium on hard soils-soft rocks* (pp. 799-804). Napoles: Ed. A. Evangelista.
- Roscoe, K., & Burland, J.B. (1968). On the generalised stress strain behaviour on wet clay. In J. Heyman & F. Leckie (Eds.), *Engineering plasticity* (pp. 535-609). Cambridge University Press.
- Schofield, A.N. (1993). Original cam-clay. In *International Conference on Soft Soil Engineering*. Guangzhou. Retrieved in February 20, 2022, from [http://www-civ.eng.cam.ac.uk/geotech\\_new/publications/TR/TR259.pdf](http://www-civ.eng.cam.ac.uk/geotech_new/publications/TR/TR259.pdf).
- Skempton, A.W. (1953). The colloidal activity of clays. In *Proceedings of the 3 th International Conference of Soil Mechanics and Foundation Engineering* (pp. 57-60). Switzerland: ICOSOMEF.
- Studer, B. (1827). Geognostische Bemerkungen uber einige Theile der nordlichen Alpenkette. *Zeitschr. fur Mineralogie*, 1, 1-52.
- Velasco, C. (2016). *Historia documental de los proyectos de enlace fijo del Estrecho de Gibraltar*. SECEGSA.
- Wood, D.M. (1990). *Soil behaviour and critical state soil mechanics*. Cambridge University Press. <https://doi.org/10.1017/CBO9781139878272>